Published OnlineFirst July 3, 2019; DOI: 10.1158/1535-7163.MCT-18-1216

Molecular Cancer Therapeutics

Anti-GPRC5D/CD3 Bispecific T-Cell–Redirecting Antibody for the Treatment of Multiple Myeloma

Tatsushi Kodama[1,2], Yu Kochi[3], Waka Nakai[2], Hideaki Mizuno[2], Takeshi Baba[2], Kiyoshi Habu[2], Noriaki Sawada[2], Hiroyuki Tsunoda[2], Takahiro Shima[3], Kohta Miyawaki[3], Yoshikane Kikushige[3], Yasuo Mori[3], Toshihiro Miyamoto[3], Takahiro Maeda[4], and Koichi Akashi[3,4]

Abstract

Although treatment advances over recent decades have significantly improved survival of patients with multiple myeloma, there is still an unmet medical need for more effective treatments. In this study, we identified G-protein–coupled receptor family C group 5 member D (GPRC5D) expression on the surface of malignant cells involved in multiple myeloma, but except for plasma cells and B cells, not at appreciable levels on normal hematopoietic cells and bone marrow progenitors, including hematopoietic stem cells. In addition, we constructed IgG-based anti-GPRC5D/CD3 bispecific T-cell–redirecting antibodies (GPRC5D TRAB), which suppressed the tumor growth of GPRC5D-positive myeloma cells through the activation of T cells *in vitro* and *in vivo* in xenograft models. Collectively, these findings suggest that GPRC5D is an antigen specific to multiple myeloma and a potential target of TRAB therapy.

Introduction

Multiple myeloma is the second most common hematologic malignancy, characterized by uncontrolled proliferation and accumulation of monoclonal plasma cells in the bone marrow and resulting in the overproduction of monoclonal immunoglobulin and osteolysis and end-organ damage (1, 2). Treatment advances over recent decades have significantly improved survival of patients with multiple myeloma and the FDA recently approved the first two mAbs, daratumumab and elotuzumab, which target CD38 and SLAMF7 (CS1), respectively (3–5). Nevertheless, multiple myeloma is still considered incurable malignancy; patients eventually relapse or become refractory to all available therapies or discontinue treatment due to toxicity. Thus, patients with multiple myeloma still need for more effective and well-tolerated treatments.

Therapies that direct T cells to tumors, including bispecific T-cell–redirecting antibody (TRAB) and chimeric antigen receptor (CAR)-T-cell therapies targeting CD19, have produced deep responses in patients with $CD19^+$ hematologic malignancies (6–8). The anti-CD19/CD3 bispecific TRAB blinatumomab was approved by the FDA for the treatment of relapsed/refractory B-cell precursor acute lymphocytic leukemia (B-ALL) in 2017 (9). The anti–CD19 CAR-T-cell therapy tisagenlecleucel, formerly known as CTL019, was approved by the FDA for the treatment of relapsed/refractory B-ALL in 2017 (9) and relapsed/refractory large B-cell lymphoma in 2018 (9). Another anti–CD19 CAR-T-cell therapy, axicabtagene ciloleucel, formerly known as KTE-C19 was approved by the FDA for the treatment of relapsed/refractory large B-cell lymphoma in 2017 (9). Very recently, the anti–B-cell maturation antigen (BCMA) CAR-T-cell therapy bb2121 has demonstrated sustained efficacy in relapsed/refractory patients with multiple myeloma (10). However, these TRAB and CAR-T-cell therapies also induced cytokine release syndrome, neurotoxicity, and on-target off-tumor effects resulting from the recognition of normal cells (6–10).

G-protein–coupled receptor family C group 5 member D (GPRC5D) is an orphan receptor and a seven-pass membrane protein (11). High mRNA expression of *GPRC5D* was observed in patients with multiple myeloma, whereas only low expression was detected in normal tissues (11). In addition, mRNA expression of *GPRC5D* showed a significant correlation with poor overall survival rates, and with genetic alteration such as deletion of chromosome 13q14 and translocation t(4;14) (11). However, there was no way of investigating the cell surface expression of GPRC5D on malignant cells from patients with multiple myeloma or on normal hematologic cells because, as reported by Frigyesi and colleagues, the available antibodies could not detect GPRC5D (12). In our study, we determined the cell surface expression of GPRC5D on malignant and normal hematologic cells. In addition, we evaluated the antitumor activity and mechanism of GPRC5D TRABs *in vitro* and *in vivo* in mouse models.

Materials and Methods

Clinical samples

The bone marrow of adult patients with multiple myeloma diagnosed according to WHO criteria were used in this study.

[1]Chugai Pharmabody Research Pte. Ltd., Singapore. [2]Research Division, Chugai Pharmaceutical Co., Ltd., Kamakura, Kanagawa, Japan. [3]Department of Medicine and Biosystemic Science, Kyushu University Graduate School of Medical Sciences, Fukuoka, Japan. [4]Center for Cellular and Molecular Medicine, Kyushu University Hospital, Fukuoka, Japan.

Note: Supplementary data for this article are available at Molecular Cancer Therapeutics Online (http://mct.aacrjournals.org/).

Corresponding Author: Tatsushi Kodama, Chugai Pharmabody Research Pte. Ltd., 3 Biopolis Drive, #07-11 to 16 Synapse, Singapore 138623, Singapore. Phone: 65-6933-4860; Fax: 65-6684-2257; E-mail: kodama-t@chugai-pharmabody.com

Mol Cancer Ther 2019;18:1555–64

doi: 10.1158/1535-7163.MCT-18-1216

Published OnlineFirst July 3, 2019; DOI: 10.1158/1535-7163.MCT-18-1216

Supplementary Table S1 summarizes the characteristics of the patients with multiple myeloma analyzed in this study. Human adult bone marrow and peripheral blood samples were also obtained from healthy donors. Cord blood cells were obtained from full-term deliveries (provided by the Ishida Ladies Clinic, Fukuoka, Japan). Written informed consent was obtained from all patients and volunteers in accordance with the Declaration of Helsinki of 1975, as revised in 1983. The Institutional Review Board of Kyushu University Hospital (Fukuoka, Japan) approved all research on human subjects.

Cell lines

NCI-H929 and OPM-2 cells from DSMZ; KMS-34, KMS-26, and KMS-28BM cells from Human Science; NCI-H1975 cells were obtained from ATCC; and GloResponse NFAT-luc2 Jurkat cells were obtained from Promega. Each cell line was cultured using the medium recommended by the suppliers.

Generation of Chinese hamster ovary cells expressing human GPRC5D

Human GPRC5D with c-myc tag at N terminal was subcloned into the pCXND3 vector (13). The plasmid was linearized for transfection at a unique Pvu I site. Chinese hamster ovary (CHO) cells were cultured in CHO-S-FM II (Invitrogen) supplemented with 1% HT Supplement (Invitrogen), and penicillin/streptomycin (Invitrogen) at 37°C, 5% CO_2. To obtain CHO cells expressing GPRC5D, 20 μg of expression vector was transfected by the electroporation method using GenePulser Xcell (Bio-Rad) under conditions of 1.5 kV and 25 μFD. Appropriate cells were identified for selection in 500 μg/mL of geneticin (Invitrogen). Anti-myc mAb (Sigma-Aldrich) was used for the GPRC5D expression of resistant clones by flow cytometer (LSRFortessa, BD Biosciences), and CHO cells expressing of human GPRC5D were established for subsequent experiments.

Generation of GPRC5D-specific recombinant mAbs

All animal care and experimental protocols were performed in accordance with the guidelines for the care and use of laboratory animals at Chugai Pharmaceutical Co., Ltd. The protocol was approved by the Institutional Animal Care and Use Committee (IACUC) at Chugai Pharmaceutical Co., Ltd. Twelve New Zealand white rabbits (Kitayama Labes) were immunized seven times with purified plasmid DNA of pCXND3 vector carrying human *GPRC5D* cDNA according to the general protocol for DNA immunization (14). B cells able to produce anti-GPRC5D antibodies were identified by flow cytometer and their genes were sequenced for antibody-variable regions (15). To construct rabbit anti-GPRC5D antibodies and chimeric anti-GPRC5D antibodies, the DNA segment encoding each rabbit's Ig variable region was inserted into an expression vector containing the constant region of rabbit IgG/kappa, mouse IgG1/kappa, or modified human IgG1/kappa for Fab-arm exchange. Expression vectors transfected into FreeStyle293 cells were expressed as recombinant IgGs, which were then purified from culture supernatants using rProtein A-Sepharose (GE Healthcare). GPRC5D TRABs were generated by Fab-arm exchange as described previously (16).

Flow cytometry

Mononuclear cells (MNC) from patients with multiple myeloma or healthy donors were concentrated by standard gradient centrifugation, and $CD34^+$ cells were enriched from MNCs by using the Indirect CD34 MicroBead Kit (Miltenyi Biotec). Dead cells were excluded by propidium iodide (PI) staining. Appropriate isotype-matched, irrelevant control mAbs were used to determine the level of background staining. Cells were stained with a PerCP/Cy5.5-conjugated lineage cocktail, including anti-CD3 (UCHT1), CD4 (SK3), CD8 (SK1), CD10 (HI10a), CD19 (HIB19), CD20 (2H7), CD11b (ICRF44), CD14 (HCD14), CD56 (HCD56) and CD235ab (HIR2), FITC-conjugated anti-CD138 (MI15), anti-CD45RA (HI100) or anti-CD3 (UCHT1), PE-conjugated anti-rabbit IgG (polyclonal), APC-conjugated anti-CD34 (8G12), anti-CD38 (HIT2), anti-CD11b (ICRF44) or anti-CD19 (HIB19), BV510-conjugated anit-CD14 (M5E2), Pacific blue–conjugated anti-CD56 (HCD56), BV421-conjugated anti-CD38 (HIT2), APC/Cy7-conjugated anti-CD45 (HI30) or anti-CD16 (3G8), PE/Cy7-conjugated anti-CD19 (HIB19), biotinylated anti-IL-3RA (6H6), or rabbit anti-GPRC5D antibody (GPA0039). Streptavidin-conjugated PE-Cy7 was used for visualization of the biotinylated antibodies (BD Pharmingen, BioLegend). Goat anti-human IgG Fc conjugated with DyLight488 (Thermo Fisher Scientific) was used as a secondary antibody for detection.

CHO cells expressing GPRC5D and parent CHO cells were stained with the following recombinant mAbs: rabbit anti-GPRC5D antibodies and GPRC5D TRABs. Goat anti-human IgG Fc conjugated with DyLight488 (Thermo Fisher Scientific) was used as a secondary antibody for detection.

The expression of cell surface antigens was analyzed by flow cytometry (FACSAria or LSRFortessa, BD Biosciences) using FlowJo software (Tree Star). The cell surface density of GPRC5D on each cancer cell line was quantified by a FACSVerse Cytometer (BD Biosciences) with a mouse anti-GPRC5D antibody and QIFIKIT (Dako) according to the manufacturer's instructions.

Affinity measurement

The equilibrium dissociation constant (K_D) values of binding curves in flow cytometry were determined by a one-site–specific binding model (GraphPad Software, Inc.).

The binding affinity of antibodies at pH 7.4 was determined at 37°C using a Biacore T200 Instrument (GE Healthcare). Recombinant Streptavidin (Genscript) was immobilized on each flow cell of a CM4 sensor chip using an Amine Coupling Kit (GE Healthcare). Human CD3ε peptide (biotinylated) was prepared in HBS-EP+ buffer [10 mmol/L HEPES, 150 mmol/L NaCl, 3 mmol/L EDTA, 0.005% Tween 20 (pH7.4)] and was captured at 10–20 resonance unit (RU) onto the Streptavidin surface. Antibodies were prepared in buffer [20 mmol/L ACES, 150 mmol/L NaCl, 0.05% Tween 20, 0.005% NaN3 (pH7.4)]. Each antibody was injected at 130 nmol/L and 520 nmol/L, followed by dissociation. The sensor surface was regenerated each cycle with 10 mmol/L Glycine-HCl pH 2.0. The binding affinity was determined by processing and fitting the data to a 1:1 binding model using Biacore T200 Evaluation software, version 2.0 (GE Healthcare).

Microarray analysis

Bone marrow samples from patients with multiple myeloma were investigated with a Sentrix BeadChip Assay for Gene Expression and HumanHT-12 v4 (Illumina), as in our previous study (17).

Cell lysis and cytokine assay

T-cell activation was measured by Bio-Glo Luciferase Assay System (Promega) using GloResponse NFAT-luc2 Jurkat cells as

Published OnlineFirst July 3, 2019; DOI: 10.1158/1535-7163.MCT-18-1216

effector cells and cancer cells or normal cells as target cells. A total of 12,500 target cells and 75,000 effector cells were seeded in 96-well white culture plates with varying concentrations of antibody for 24 hours at 37°C and 5%CO_2.

T-cell–dependent cell cytotoxicity was evaluated by LDH assay using human peripheral blood mononuclear cells (PBMC) as effector cells and cancer cell lines as target cells. Human PBMCs were isolated from the fresh blood of healthy donors using Ficoll-Paque PLUS (GE Healthcare). A total of 10,000 target cells and 100,000 human PBMCs were seeded into each well of a 96-well U-bottom plate and incubated with various antibody concentrations for 24 hours at 37°C and 5%CO_2. Target cell killing was measured by an LDH Cytotoxicity Detection Kit (Takara Bio).

Cytokine concentrations from supernatants of the T-cell cytotoxicity assay were quantified by a BD FACSVerse cytometer using a BD Cytometric Bead Array (CBA) Human Th1/Th2 Cytokine Kit II (BD Biosciences) according to the manufacturer's instructions.

In vivo efficacy studies

All animal experiments in this study were performed in accordance with protocols approved by the IACUC of Chugai Pharmaceutical Co., Ltd.

To investigate NCI-H929 or KMS-26 tumors in mice inoculated with human T cells, NOD-SCID mice were obtained from CLEA Japan, Inc. A total of 1.0×10^7 cells/mouse of NCI-H929 or KMS-26 cells were grown as subcutaneous tumors in NOD-SCID mice. Mice were randomized to receive 0.2 mg/mouse of anti-Asialo GM1 Antibody (Wako Pure Chemicals). Human T cells were prepared from human PBMCs using Dynabead Human T-Activator CD3/CD28 (Thermo Fisher Scientific), and 3.0×10^7 cells/mouse of human T cells were intraperitoneally injected into mice as effector cells. A total of 10 mg/kg of each antibody was intravenously administered 5 hours after T-cell injection. The length (L) and width (W) of the tumor mass were measured twice per week, and tumor volume (TV) was calculated as: $TV = (L \times W^2)/2$.

To investigate NCI-H929 tumors in a humanized NOG mouse model, NOG mice were obtained from In-Vivo Science Inc. A total of 5.0×10^4 cells of human cord blood–derived $CD34^+$ hematopoietic stem cells (HSC) were injected intravenously 24 hours after irradiation. Thirteen weeks later, 8.0×10^6 NCI-H929 cells were grown as subcutaneous tumors in NOG mice. Ten days after tumor implantation, mice were randomized to intravenously receive 10 mg/kg of each antibody. Tumor size was measured twice per week.

mRNA expression analysis using xenograft tumors

Total RNA was analyzed by using the nCounter Human Immunology v2 Expression panel (Nanostring), which assesses the expression of 594 human immunology-related genes. Each mRNA expression profile was $\log_2$-transformed and mean-centered. Then, for each gene, expression changes to control were calculated by subtracting the median value of nontreated samples. Hierarchical clustering was conducted for genes using Pearson correlation distance. R 3.4.3 (https://www.r-project.org/) was used for data analysis and visualization.

mRNA expression data in normal tissues

mRNA expression data in normal tissues were obtained from the GTEx Portal (dbGaP accession number phs000424.v7.p2) on October 26, 2018.

Results

Identification of GPRC5D as a multiple myeloma–specific antigen and establishment of mAbs against human GPRC5D

To identify myeloma-specific antigens, we first performed microarray analysis using $CD138^+$ $CD38^{high}$ $CD45^-$ $CD19^-$ $CD56^+$ malignant cells from patients with multiple myeloma ($n = 8$) and normal human $CD19^+$ B cells from the peripheral blood of healthy donors ($n = 7$). In this analysis, we found that *GPRC5D* was highly expressed in malignant cells, but very weakly or not at all in normal B cells (Fig. 1A), consistent with previous reports (11, 12). However, there was no evidence of the cell surface expression of GPRC5D on malignant cells from patients with multiple myeloma because, as mentioned by Frigyesi and colleagues, available antibodies could not detect GPRC5D (12). Thus, to clarify the cell surface expression of GPRC5D, we established specific mAbs against human GPRC5D: GPA0018, GPA0021, GPA0032, and GPA0039. All four showed binding activity to CHO cells expressing human GPRC5D (Fig. 1B and C).

Identification of the cell surface expression of GPRC5D on myeloma cells

Next, to investigate the cell surface expression of GPRC5D on malignant cells from patients with multiple myeloma, we conducted flow cytometry analysis using our GPRC5D antibody GPA0039 against both malignant cells and normal B cells. Consistent with the mRNA expression of *GPRC5D* confirmed by our microarray analysis, the cell surface expression of GPRC5D was observed on malignant cells from a patient with multiple myeloma (Fig. 2A, patient number MM#1 in Supplementary Table S1), but hardly observed on normal $CD19^+$ B cells from a healthy donor (Fig. 2B). Analysis of malignant cells from 11 patients with multiple myeloma and B cells from 3 healthy donors revealed a higher proportion of GPRC5D-positivity in 9 of 11 (82%) malignant cells compared with the highest proportion detected in the normal B cells (Fig. 2C). In addition, the cell surface expression level of GPRC5D in most individuals was similar to that of the NCI-H929 myeloma cell line (Fig. 2A and D; Supplementary Fig. S1). To reveal whether GPRC5D expression was tumor specific, we first looked for its expression on normal human hematopoietic cells. We found that, except for plasma cells, normal $CD3^+$ T cells, $CD56^+$ NK cells, $CD14^+$ monocytes, and $CD11b^+$ granulocytes all lacked the expression of GPRC5D protein on their surfaces (Fig. 2E and F). Next, we investigated its possible expression on a variety of bone marrow progenitors, including HSCs and the following downstream progenitors: common myeloid progenitor (CMP), granulocyte/monocyte progenitor (GMP), megakaryocyte/erythrocyte progenitor (MEP), and pro-B cells. We found that human $CD34^+$ $CD38^-$ lineage-negative (lin^-) HSCs completely lacked GPRC5D expression, and that $CD34^+$ $CD38^+$ myeloid and the lymphoid progenitors CMP, GMP, MEP, and pro-B cells were also negative (Fig. 2G). These results suggest that GPRC5D is specifically expressed on the cell surfaces of malignant cells in patients with multiple myeloma.

GPRC5D TRABs ligated human $CD3^+$ T cells and GPRC5D-expressing cells, leading to the activation of human T cells

Having identified the specific expression of GPRC5D on malignant cells, we felt that killing those specific cells by targeting GPRC5D would show a promising therapeutic approach to the disease. To investigate whether GPRC5D could be therapeutic

Published OnlineFirst July 3, 2019; DOI: 10.1158/1535-7163.MCT-18-1216

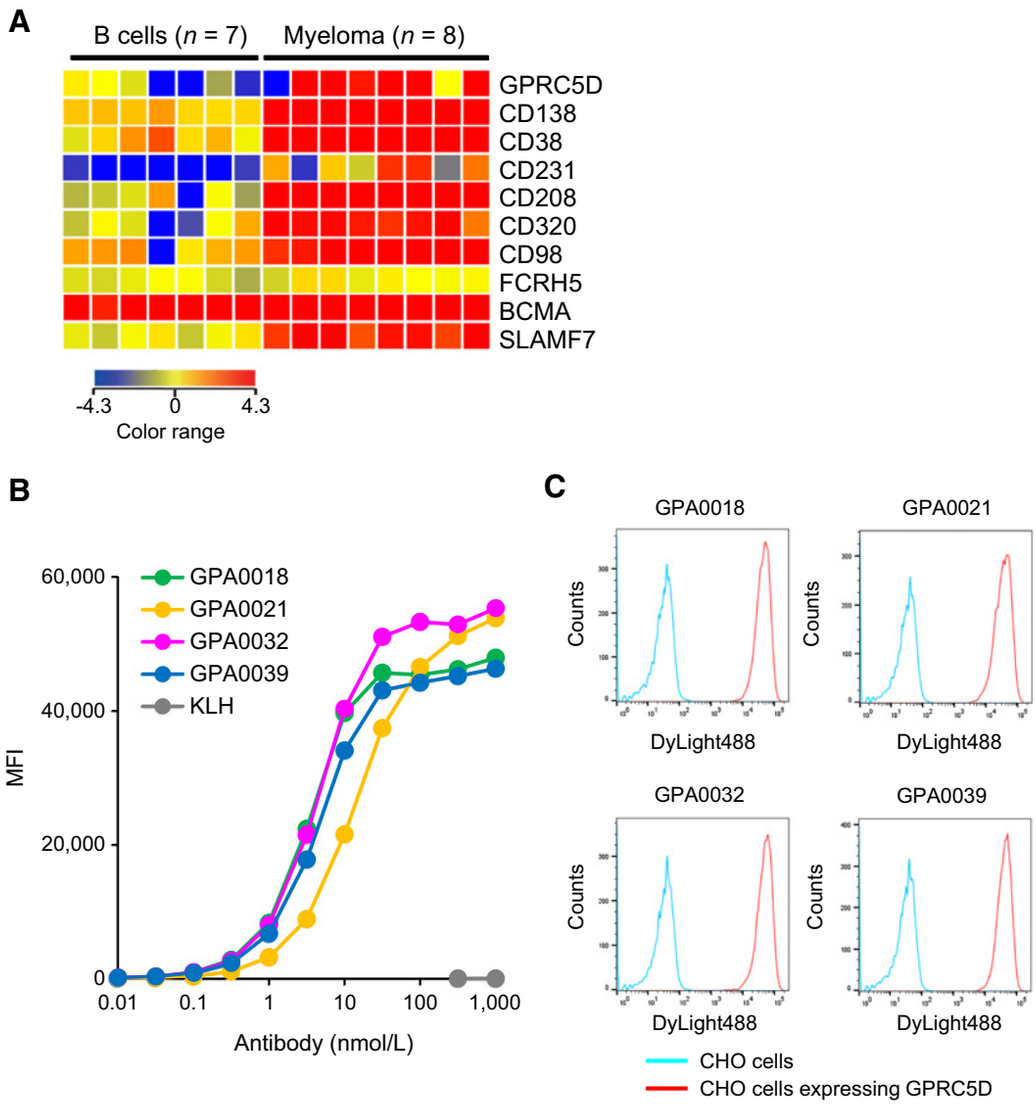

Figure 1.

Selection of GPRC5D as an antigen specific to multiple myeloma and generation of anti-GPRC5D antibodies. **A,** Microarray analysis of the $CD19^+$ normal B cells and $CD138^+$ $CD38^{high}$ $CD45^-$ $CD19^-$ $CD56^+$ myeloma cells. **B,** Binding activity of various concentrations of anti-GPRC5D antibodies on CHO cells expressing GPRC5D plotted as median fluorescence intensity (MFI). **C,** Binding activity of 32 nmol/L of anti-GPRC5D antibodies on CHO cells expressing GPRC5D or parental CHO cells plotted as histogram.

target, we generated four GPRC5D TRABs (GPA0018 TRAB, GPA0021 TRAB, GPA0032 TRAB, and GPA0039 TRAB) with different CDR sequences in GPRC5D-binding arms (Supplementary Table S2). For the heavy-chain constant region, L235R/S239K/N297A (in EU numbering) mutations were introduced into the CH2 region of IgG1 antibody to abolish binding to Fcγ receptors (18). These mutations were introduced to avoid GPRC5D-independent activity caused by Fcγ receptors and CD3-expressing cells.

To confirm the binding affinity of the GPRC5D TRABs to GPRC5D, we performed flow cytometry analysis using CHO cells expressing human GPRC5D. All four GPRC5D TRABs bound to GPRC5D. GPA0018 TRAB and GPA0039 TRAB showed stronger binding affinity than GPA0021 TRAB and GPA0032 TRAB (Fig. 3A). The binding affinity (K_D value) of GPA0018 TRAB and GPA0039 TRAB to GPRC5D was 4.9 and 7.4 nmol/L, respectively (flow cytometry analysis), while the K_D value of both to CD3ε was 94 to 100 nmol/L (surface plasmon resonance measurement).

To investigate T-cell activation and the simultaneous binding to both GPRC5D-expressing cancer cells and $CD3^+$ T cells, we used a luciferase assay system with GloResponse NFAT-luc2 Jurkat cells as effector cells and GPRC5D-expressing human multiple myeloma cell line NCI-H929 as cancer cells (Supplementary Fig. S2A). All four GPRC5D TRABs cross-linked T cells to GPRC5D-expressing cancer cells, leading to the activation of the CD3 downstream signaling pathway. The activation by GPA0018 TRAB and GPA0039 TRAB was much stronger than that of GPA0021 TRAB and GPA0032 TRAB (Fig. 3B), consistent with their binding

Published OnlineFirst July 3, 2019; DOI: 10.1158/1535-7163.MCT-18-1216

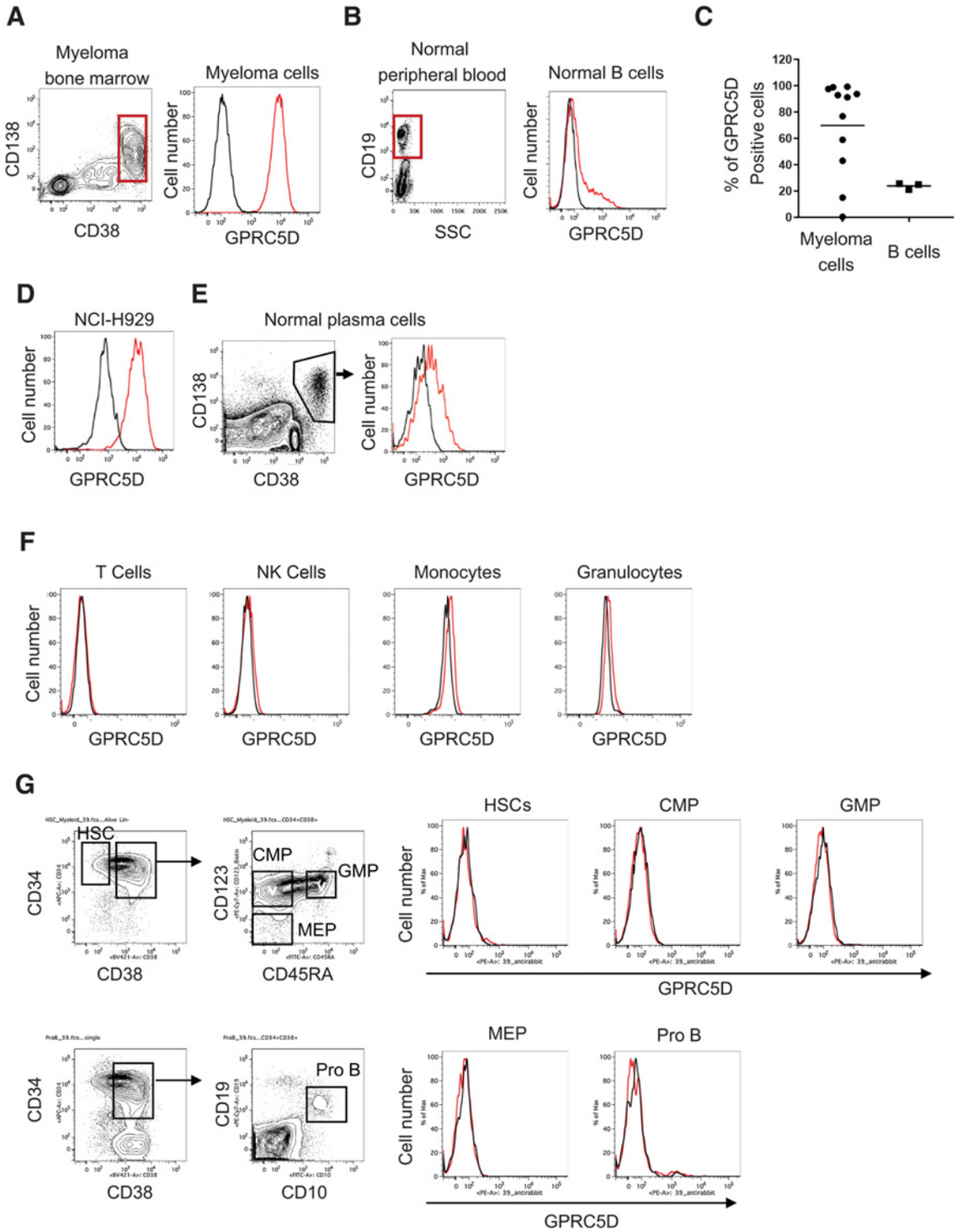

Figure 2.

Cell surface expression of GPRC5D on malignant cells from multiple myeloma and normal hematopoietic cells. Flow cytometry results show the cell surface expression of GPRC5D on malignant cells from a multiple myeloma (**A**, patient number: MM#1 in Supplementary Table S1) and normal B cells from a healthy donor (**B**). **C,** Summary of proportion of GPRC5D positivity on malignant cells from 11 patients with multiple myeloma and on B cells from three healthy donors. Flow cytometry results show the expression of GPRC5D on NCI-H929 (**D**), normal plasma cells (**E**), normal $CD3^+$ T cells, $CD56^+$ NK cells, $CD14^+$ monocytes, and $CD11b^+$ granulocytes from peripheral blood (**F**), and hematopoietic stem and progenitor cells (**G**). Black lines indicate staining with a control IgG1 antibody, and red lines indicate staining with GPA0039.

Published OnlineFirst July 3, 2019; DOI: 10.1158/1535-7163.MCT-18-1216

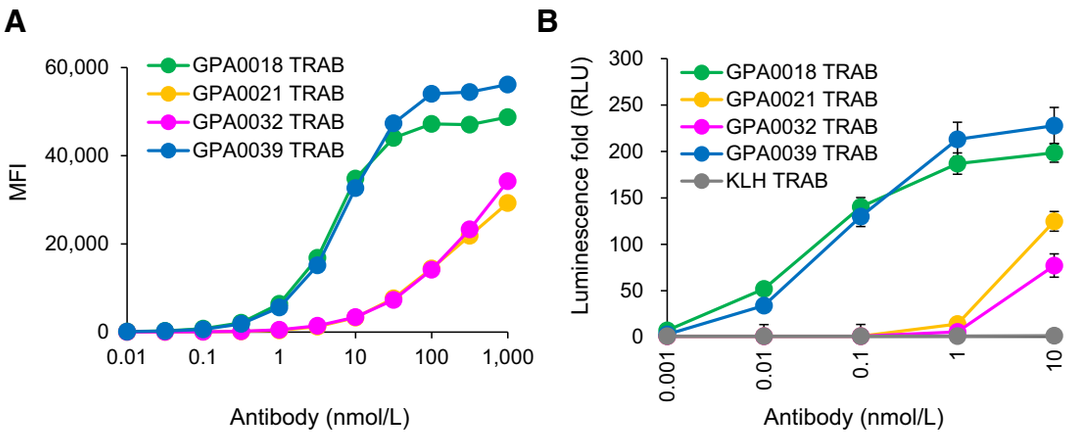

Figure 3.

Functional analysis of GPRC5D TRABs. **A,** Flow cytometry results show the binding activity of GPRC5D TRABs to CHO cells expressing GPRC5D. Green line indicates GPA0018 TRAB, orange line indicates GPA0021 TRAB, pink line indicates GPA0032 TRAB, and blue line indicates GPA0039 TRAB. **B,** T-cell activation of GPRC5D TRABs after coculturing with GloResponse NFAT-luc2 Jurkat cells and GPRC5D-expressing NCI-H929 myeloma cells. Green line indicates staining with GPA0018 TRAB, orange line indicates GPA0021 TRAB, pink line indicates GPA0032 TRAB, blue line indicates GPA0039 TRAB, and gray line indicates KLH TRAB as a negative control. Results are expressed as relative fold change compared with no antibody control.

activity. These results suggest that our novel GPRC5D TRABs efficiently ligate human $CD3^+$ T cells and GPRC5D-expressing cells, activating *in vitro* human T cells in a manner dependent on their affinity to GPRC5D.

GPRC5D TRABs mediated target-dependent cell cytotoxicity via activation of human T cells

After confirming that GPRC5D TRABs could ligate both human $CD3^+$ T cells and GPRC5D-expressing cells, and that GPA0018 TRAB and GPA0039 TRAB had a much stronger effect, we then evaluated the cytotoxicity of GPA0018 TRAB and GPA0039 TRAB against GPRC5D-expressing multiple myeloma cell lines and a GPRC5D-negative cancer cell line. With unstimulated human PBMCs, both GPA0018 TRAB and GPA0039 TRAB induced the cytotoxicity against GPRC5D-expressing multiple myeloma cell lines (NCI-H929, OPM-2, KMS-34, KMS-26, and KMS-28BM) but none against GPRC5D-negative lung cancer cell line NCI-H1975 (Fig. 4A; Supplementary Fig. S2A). In addition, no cytotoxicity was observed against GPRC5D-expressing NCI-H929 without the presence of human PBMCs (Supplementary Fig. S2B), suggesting the cytotoxicity of GPRC5D TRABs was mediated by effector cells in a GPRC5D-dependent manner. However, GPRC5D expression level did not strongly impact cytotoxicity induced by GPRC5D TRABs. Moreover, to provide evidence that GPRC5D TRABs activated effector cells, we evaluated cytokine secretion after adding GPA0018 TRAB or GPA0039 TRAB to cocultures of GPRC5D-expressing NCI-H929 cells and human PBMCs. Both GPA0018 TRAB and GPA0039 TRAB induced a number of cytokines: IFNγ, TNF, IL10, IL6, IL4, and IL2 (Fig. 4B). To confirm which T cells showed cytotoxicity, we evaluated the cytotoxicity of GPRC5D TRABs using purified $CD8^+$ T cells and $CD4^+$ T cells as effector cells. We confirmed that the $CD8^+$ T cells and $CD4^+$ T cells showed cytotoxicity in the presence of GPRC5D TRABs that target GPRC5D-expressing NCI-H929 cells (Supplementary Fig. S3), consistent with the previous result on GPC3 TRAB (18). Taken together, these results indicate that cytotoxicity against GPRC5D-expressing multiple myeloma cells is mediated by GPRC5D TRABs in a T-cell–dependent manner.

Antitumor activity of GPRC5D TRABs against GPRC5D-expressing multiple myeloma in mouse models

To evaluate the *in vivo* antitumor activity of GPRC5D TRABs against multiple myeloma, we used mouse xenograft tumors of GPRC5D-expressing NCI-H929 and KMS-26 cells in NOD-SCID mice inoculated with human T cells. After the tumor volume reached around 200 mm^3, the mice were treated using GPA0018 TRAB and GPA0039 TRAB as GPRC5D binders and KLH TRAB as a negative control. Treatment with a single intravenous administration of 10 mg/kg of GPA0018 TRAB led to significant reduction in the volume of both NCI-H929 and KMS-26 tumors compared with 10 mg/kg of KLH TRAB (Fig. 5A and B). Similar results were observed with a single administration of 10 mg/kg of GPA0039 TRAB (Fig. 5A and B). By the end of the NCI-H929 study, 3/8 mice treated with GPA0018 TRAB and 4/8 mice treated with GPA0039 TRAB were tumor free (Fig. 5A). One mg/kg of GPA0039 TRAB also led to a significant reduction in the volume of NCI-H929 tumors (Supplementary Fig. S4A).

To further investigate the *in vivo* antitumor activity of GPRC5D TRAB, we utilized immunocompromised NOG mice engrafted with human $CD34^+$ HSCs as in a previous study (18). A single dose of 10 mg/kg of GPA0039 TRAB or KLH TRAB was administered intravenously 10 days after the inoculation of NCI-H929 cancer cells and 13 weeks after human HSC injection. Compared with KLH TRAB, GPA0039 TRAB resulted in significant antitumor activity: 3/5 mice showed remarkable tumor regression (Fig. 5C). GPA0039 TRAB and KLH TRAB achieved comparable plasma concentrations at day 4 and day 15 in NCI-H929 tumors in a humanized NOG mouse model, suggesting that GPA0039 TRAB would not cause antigen-dependent clearance in mice (Supplementary Fig. S4B).

To understand the antitumor mechanism of GPRC5D TRAB against the NCI-H929 tumor in this humanized NOG mouse model, total RNA was extracted from the tumor at 3 days after treatment of GPA0039 TRAB or KLH TRAB, and gene expression was analyzed using the nCounter Human Immunology v2 Expression panel of 594 immune-related genes. The majority of genes upregulated by GPA0039 TRAB were immune activation genes

Published OnlineFirst July 3, 2019; DOI: 10.1158/1535-7163.MCT-18-1216

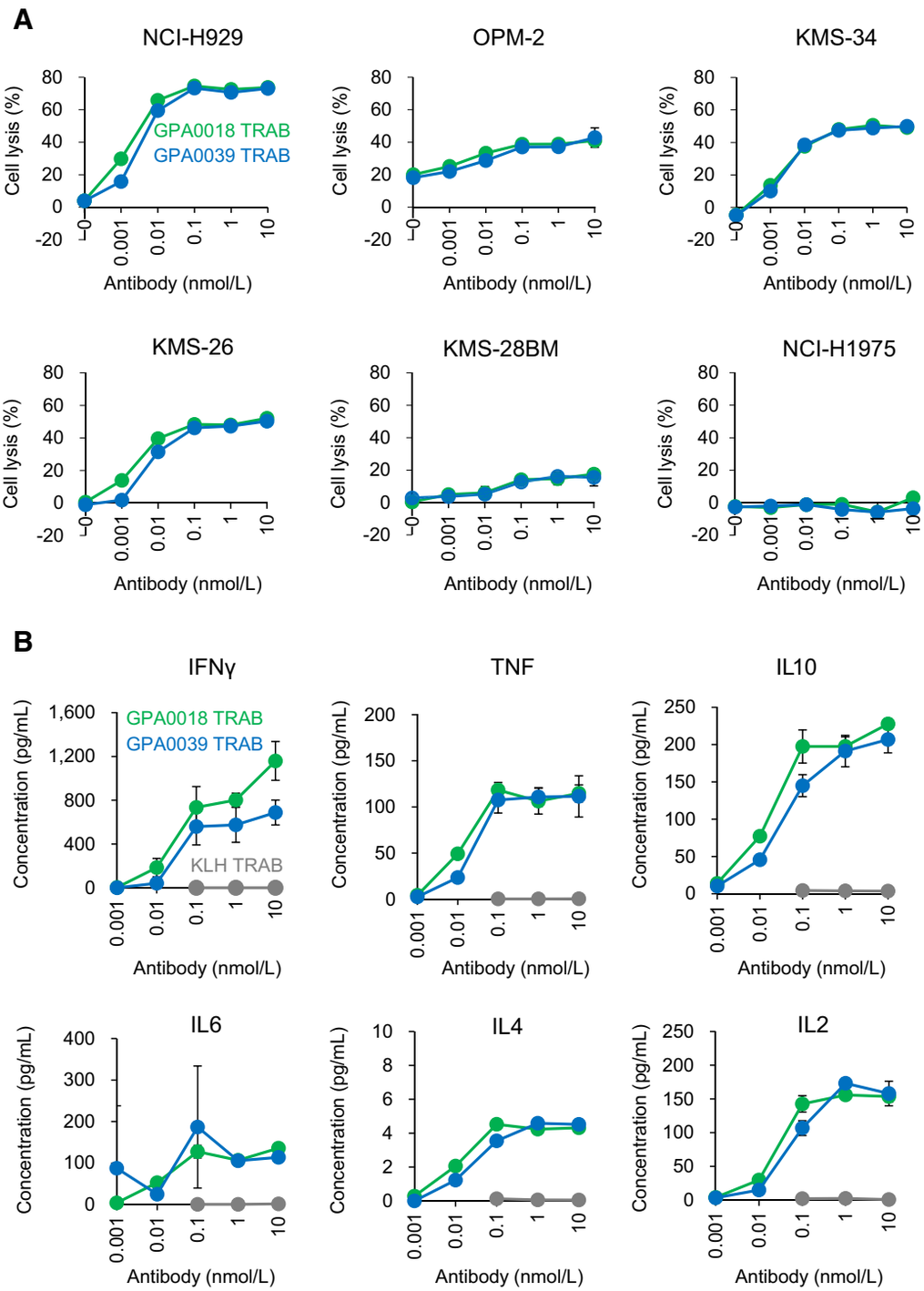

Figure 4.

Cytotoxicity and cytokines induction activity by GPRC5D TRABs against cancer cell lines. **A,** Cytotoxicity of GPRC5D TRABs when coculturing NCI-H929, OPM-2, KMS-34, KMS-26, KMS-28BM, or NCI-H1975 cells with human PBMCs. Cytotoxicity was measured via release of LDH 1 day after treatment. Green lines indicate GPA0018 TRAB, and blue lines indicate GPA0039 TRAB. Data are shown as mean ± SD ($n = 3$/group). **B,** Secretion of cytokines by the GPRC5D TRABs when coculturing NCI-H929 cells with human PBMCs. Secreted cytokines in the supernatants after 24-hour culture were quantified by CBA Human Th1/Th2 Cytokine kit II. Green lines indicate GPA0018 TRAB, blue lines indicate GPA0039 TRAB, and gray lines indicate KLH TRAB. Data are shown as mean ± SD ($n = 3$/group).

Published OnlineFirst July 3, 2019; DOI: 10.1158/1535-7163.MCT-18-1216

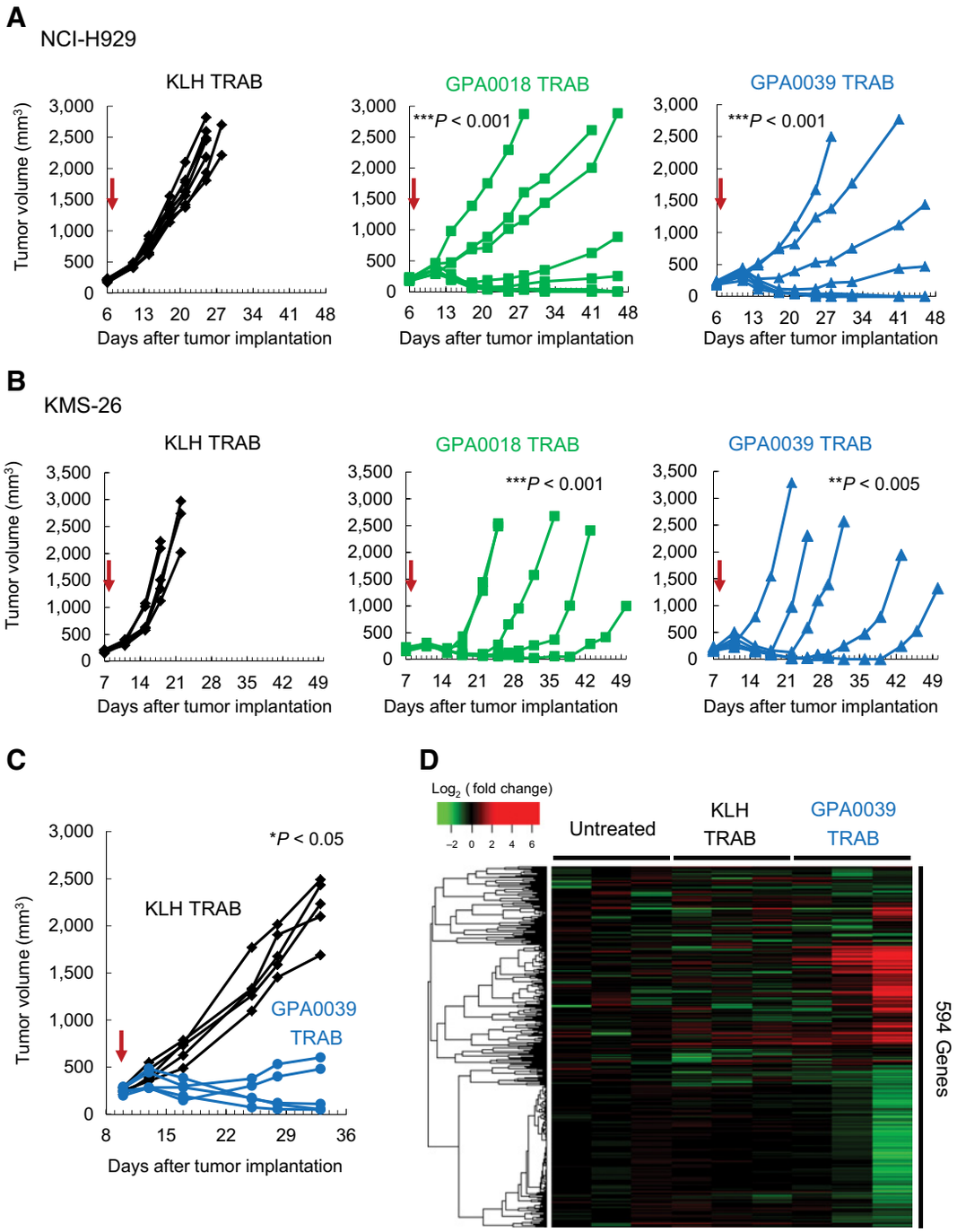

Figure 5.

Antitumor activity of GPRC5D TRABs against multiple myeloma in mouse models. **A,** Antitumor activity of GPA0018 TRAB, GPA0039 TRAB, or KLH TRAB against NCI-H929 tumors in NOD-SCID mouse inoculated with human T cells. Black lines indicate KLH TRAB, green lines indicate GPA0018 TRAB, and blue lines indicate GPA0039 TRAB. Arrows indicate timing of TRAB administration. Parametric Dunnett test: ***, $P < 0.001$, versus KLH TRAB treatment at day 25. **B,** Antitumor activity of GPA0018 TRAB, GPA0039 TRAB, or KLH TRAB against KMS-26 tumors in NOD-SCID mice inoculated with human T cells. Black lines indicate KLH TRAB, green lines indicate GPA0018 TRAB, and blue lines indicate GPA0039 TRAB. Arrows indicate timing of TRAB administration. Parametric Dunnett test: ***, $P < 0.001$; **, $P < 0.005$, versus KLH TRAB treatment at day 18. **C,** Antitumor activity of GPA0039 TRAB or KLH TRAB against NCI-H929 in a humanized mouse model. Black lines indicate KLH TRAB, and blue lines indicate GPA0039 TRAB. Arrows indicate timing of TRAB administration. Wilcoxon test: *, $P < 0.05$, versus KLH TRAB treatment at day 33. **D,** Gene expression analysis in NCI-H929 tumors in a humanized mouse model. RNA from untreated tumors and tumors treated with KLH TRAB or GPA0039 TRAB were used for nCounter gene expression assay. Each group was tested in triplicate ($n = 3$). Heatmap shows changes in the expression of each gene (log-ratio to median value of untreated samples).

Published OnlineFirst July 3, 2019; DOI: 10.1158/1535-7163.MCT-18-1216

such as *IFNγ*, *IFNγ*-inducible chemokines *CXCL9* and *CXCL10*, and also *IL2RA*, which is expressed on activated T cells (Table 1 and Fig. 5D). Taken together, these results indicate that, in mouse models, GPRC5D TRAB exhibits potent antitumor activity against GPRC5D-expressing multiple myeloma through the activation of T cells.

Discussion

In this study, we determined that the surface of malignant cells from patients with multiple myeloma were GPRC5D positive and that, except for plasma cells and B cells, normal human hematopoietic cells such as T cells, NK cells, monocytes, granulocytes, and bone marrow progenitors including HSCs and downstream progenitors, lacked the expression of GPRC5D protein (Fig. 2). Consistent with GPRC5D expression on normal bone marrow progenitor cells, no T-cell activation by GPRC5D TRABs was detected in the presence of human bone marrow $CD34^+$ cells (Supplementary Fig. S5), suggesting that GPRC5D TRABs would not be cytotoxic to human bone marrow $CD34^+$ cells. *GPRC5D* mRNA expression in Genotype-Tissue Expression (GTEx) sample set containing 8,555 samples from 53 different human tissues was analyzed by the GTEx consortium (19, 20). The median transcripts per million (TPM) value of *GPRC5D* in each tissue was less than five, except in lung tissue (median TPM value: 5.240, $n = 427$, Supplementary Fig. S6A). Although the median TPM value of *GPRC5D* in skin was less than five, some skin tissues did express *GPRC5D*, consistent with a previous report that GPRC5D expressed in skin is involved with keratin synthesis in hair follicles (21). BCMA antigen density on malignant cells derived from 43 patients with multiple myeloma was significantly higher than on all normal bone marrow cell subsets (22), and BCMA CAR-T-cell therapy bb2121 has demonstrated sustained efficacy in relapsed/refractory patients with multiple myeloma (10). While this evidence makes BCMA an excellent target for TRAB in multiple myeloma, a *BCMA* median TPM value greater than five was observed in Epstein-Barr virus–transformed lymphocytes (median TPM value: 122.915, $n = 130$), transverse colon (median TPM value: 6.635, $n = 274$), minor salivary gland (median TPM value: 7.350, $n = 97$), the terminal ileum of the small intestine (median TPM value: 6.580, $n = 137$), and spleen (median TPM value: 18.685, $n = 162$, Supplementary Fig. S6B). Thus, GPRC5D has a highly restricted expression pattern, not only in normal hematopoietic cells, but also in normal tissues.

Table 1. Upregulated genes in GPA0039 TRAB–treated NCI-H929 xenograft tumors

Gene	Untreated	KLH TRAB	GPRC5D TRAB
IL2RA	0.04	0.09	5.36
CXCL9	0.21	0.17	4.96
CXCL10	−0.20	−0.21	4.33
IL3	0.23	−0.57	3.86
GBP1	0.15	0.38	3.53
GBP5	0.02	0.70	3.22
IL9	−0.01	0.09	3.13
LAG3	−0.02	0.18	3.02
IFNG	−0.01	0.17	2.95
LTA	−0.02	−0.12	2.58

NOTE: Mice bearing NCI-H929 tumors were intravenously administered a dose of 10 mg/kg of KLH TRAB or GPA0039 TRAB, and total RNA was extracted from the tumor at 3 days after treatment. mRNA expression was identified by nCounter Human Immunology v2 Expression panel. The top 10 upregulated genes in GPA0039 TRAB–treated samples are listed. Values indicate averaged $\log_2$-ratio to median of untreated samples for untreated ($n = 3$), KLH TRAB treated ($n = 3$), and GPRC5D TRAB–treated ($n = 3$) groups.

Safety evaluation with GPRC5D TRABs in animal models has been a challenge. For example, our anti-GPRC5D antibodies, such as GPA0018 and GPA0039, did not bind to cynomolgus monkey GPRC5D (Supplementary Fig. S7). In addition, although our GPRC5D TRABs were cross-reactive to the CD3 of both humans and cynomolgus monkeys, they were not cross-reactive to mouse CD3 (18). For these reasons, no safety studies using animals were conducted with our GPRC5D TRABs. Alternative methods of nonclinical safety evaluation should be considered for future trials. Because a separate GPRC5D TRAB (JNJ-64407564) study in patients with multiple myeloma has been started, this study will assess the safety risk.

Genetic alteration is an important prognostic parameter in multiple myeloma (23). Translocation t(4;14), observed in approximately 15% of patients with multiple myeloma, is known to be associated with poor survival (23). Some studies have demonstrated significant improvement in outcomes, including long-term survival, for patients possessing translocation t(4;14) when treated with a bortezomib-based regimen (24, 25). However, despite this treatment, translocation t(4;14) still remains a dire prognostic factor in predicting survival. In a previous report, mRNA expression of *GPRC5D* showed a significant correlation with translocation t(4;14) and poor overall survival (11). In our study, we confirmed GPRC5D cell surface expression on malignant cells derived from a patient with multiple myeloma with translocation t(4;14) (patient number: MM#3 of Supplementary Table S1 and Supplementary Fig. S1). In addition, we confirmed that GPRC5D TRABs showed strong antitumor activity in GPRC5D-positive NCI-H929 tumor models with translocation t(4;14) (26). These results suggest that patients with translocation t(4;14) may benefit from GPRC5D TRAB therapy.

In conclusion, based on the tumor-specific expression of GPRC5D and the antitumor activity of the GPRC5D TRABs, we consider GPRC5D an excellent target in the treatment of multiple myeloma, especially through TRAB therapy.

Disclosure of Potential Conflicts of Interest

Y. Kochi reports receiving a commercial research grant from Chugai Pharmaceutical Co. Ltd. No potential conflicts of interest were disclosed by the other authors.

Authors' Contributions

Conception and design: T. Kodama, H. Tsunoda, T. Shima, K. Akashi
Development of methodology: Y. Kochi, T. Shima
Acquisition of data (provided animals, acquired and managed patients, provided facilities, etc.): T. Kodama, Y. Kochi, W. Nakai, T. Baba, K. Habu, T. Shima, K. Miyawaki, Y. Kikushige
Analysis and interpretation of data (e.g., statistical analysis, biostatistics, computational analysis): T. Kodama, Y. Kochi, W. Nakai, H. Mizuno, T. Shima, Y. Kikushige
Writing, review, and/or revision of the manuscript: T. Kodama, Y. Kochi, W. Nakai, K. Habu, N. Sawada, H. Tsunoda, Y. Kikushige, Y. Mori, K. Akashi
Administrative, technical, or material support (i.e., reporting or organizing data, constructing databases): K. Habu, N. Sawada, T. Shima, T. Miyamoto
Study supervision: T. Kodama, N. Sawada, H. Tsunoda, K. Miyawaki, T. Maeda, K. Akashi

Acknowledgments

We thank N. Ikeda, N. Kimura, I. Matsuo, K. Kuramoto, S. Kuramoto, and M. Muraoka for the biological assay and the *in vivo* study. We also thank Ishida Ladies Clinic for providing cord blood samples. This work was supported, in part, by a Grant-in-Aid for Scientific Research on Innovative Areas (grant no.

Published OnlineFirst July 3, 2019; DOI: 10.1158/1535-7163.MCT-18-1216

22130001 and 22130002, to K. Akashi), a Grant-in-Aid for Challenging Exploratory Research (grant no. 24659463 and 15K15365, to K. Akashi), a Grant-in-Aid for Scientific Research (A; grant no. 25253069 and 16H02662, to K. Akashi), a Grant-in-Aid for Young Scientists (A; grant no. 26713034 and 16H06250, to Y. Kikushige), a Grant-in-Aid for Scientific Research (B; grant no. 23390254, to T. Miyamoto), Japan Agency for Medical Research and Development (AMED) grants (JP17ck0106163h0002 and JP17cm0106507h0002), Grant-in-Aid for Scientific Research S (16H06391), Grant-in-Aid for Scientific Research A (17H01567, to T. Maeda), a Grant-in-Aid for Young Scientists (16K19578, to K. Miyawaki), and a Grant-in-Aid for Scientific Research on Innovative Areas (grant no. 25115002 and 16H05340, to T. Miyamoto). This work was also supported, in part, by a contribution from Social Medical Corporation and the Chiyukai Foundation. The Genotype-Tissue Expression (GTEx) Project was supported by the Common Fund of the Office of the Director of the NIH, and by NCI, NHGRI, NHLBI, NIDA, NIMH, and NINDS. This study was funded by Chugai Pharmaceutical Co., Ltd.

The costs of publication of this article were defrayed, in part, by the payment of page charges. This article must therefore be hereby marked *advertisement* in accordance with 18 U.S.C. Section 1734 solely to indicate this fact.

Received December 3, 2018; revised April 29, 2019; accepted June 28, 2019; published first July 3, 2019.

References

1. Dimopoulos MA, Richardson PG, Moreau P, Anderson KC. Current treatment landscape for relapsed and/or refractory multiple myeloma. Nat Rev Clin Oncol 2015;12:42–54.
2. Kyle RA, Rajkumar SV. Multiple myeloma. N Engl J Med 2004;351:1860–73.
3. Phipps C, Chen Y, Gopalakrishnan S, Tan D. Daratumumab and its potential in the treatment of multiple myeloma: overview of the preclinical and clinical development. Ther Adv Hematol 2015;6:120–7.
4. Lonial S, Dimopoulos M, Palumbo A, White D, Grosicki S, Spicka I, et al. Elotuzumab therapy for relapsed or refractory multiple myeloma. N Engl J Med 2015;373:621–31.
5. Palumbo A, Sonneveld P. Preclinical and clinical evaluation of elotuzumab, a SLAMF7-targeted humanized monoclonal antibody in development for multiple myeloma. Expert Rev Hematol 2015;8:481–91.
6. Kantarjian H, Stein A, Gokbuget N, Fielding AK, Schuh AC, Ribera JM, et al. Blinatumomab versus chemotherapy for advanced acute lymphoblastic leukemia. N Engl J Med 2017;376:836–47.
7. Maude SL, Laetsch TW, Buechner J, Rives S, Boyer M, Bittencourt H, et al. Tisagenlecleucel in children and young adults with B-cell lymphoblastic leukemia. N Engl J Med 2018;378:439–48.
8. Neelapu SS, Locke FL, Bartlett NL, Lekakis LJ, Miklos DB, Jacobson CA, et al. Axicabtagene ciloleucel CAR T-cell therapy in refractory large B-cell lymphoma. N Engl J Med 2017;377:2531–44.
9. Mackall CL. Engineering a designer immunotherapy. Science 2018;359:990–1.
10. Raje NS, Berdeja JG, Lin Y, Munshi NC, Samuel D, Siegel DS, et al. bb2121 anti-BCMA CAR T-cell therapy in patients with relapsed/refractory multiple myeloma: updated results from a multicenter phase I study. J Clin Oncol 36, 2018 (suppl; abstr 8007).
11. Atamaniuk J, Gleiss A, Porpaczy E, Kainz B, Grunt TW, Raderer M, et al. Overexpression of G protein-coupled receptor 5D in the bone marrow is associated with poor prognosis in patients with multiple myeloma. Eur J Clin Invest 2012;42:953–60.
12. Frigyesi I, Adolfsson J, Ali M, Christophersen MK, Johnsson E, Turesson I, et al. Robust isolation of malignant plasma cells in multiple myeloma. Blood 2014;123:1336–40.
13. Orita T, Tsunoda H, Yabuta N, Nakano K, Yoshino T, Hirata Y, et al. A novel therapeutic approach for thrombocytopenia by minibody agonist of the thrombopoietin receptor. Blood 2005;105:562–6.
14. Wang S, Lu S. DNA immunization. Curr Protoc Microbiol 2013;31:18.3.1–18.3.24.
15. Suzuki K, Tsunoda H, Omiya R, Matoba K, Baba T, Suzuki S, et al. Structure of the plexin ectodomain bound by semaphorin-mimicking antibodies. PLoS One 2016;11:e0156719.
16. Ueda O, Wada NA, Kinoshita Y, Hino H, Kakefuda M, Ito T, et al. Entire CD3ε, δ, and γ humanized mouse to evaluate human CD3-mediated therapeutics. Sci Rep 2017;7:45839.
17. Kikushige Y, Miyamoto T, Yuda J, Jabbarzadeh-Tabrizi S, Shima T, Takayanagi S, et al. A TIM-3/Gal-9 autocrine stimulatory loop drives self-renewal of human myeloid leukemia stem cells and leukemic progression. Cell Stem Cell 2015;17:341–52.
18. Ishiguro T, Sano Y, Komatsu SI, Kamata-Sakurai M, Kaneko A, Kinoshita Y, et al. An anti-glypican 3/CD3 bispecific T cell-redirecting antibody for treatment of solid tumors. Sci Transl Med 2017;9. doi: 10.1126/scitranslmed.aal4291.
19. Consortium GT. Human genomics. The Genotype-Tissue Expression (GTEx) pilot analysis: multitissue gene regulation in humans. Science 2015;348:648–60.
20. Li J, Stagg NJ, Johnston J, Harris MJ, Menzies SA, DiCara D, et al. Membrane-proximal epitope facilitates efficient T cell synapse formation by anti-FcRH5/CD3 and is a requirement for myeloma cell killing. Cancer Cell 2017;31:383–95.
21. Inoue S, Nambu T, Shimomura T. The RAIG family member, GPRC5D, is associated with hard-keratinized structures. J Invest Dermatol 2004;122:565–73.
22. Seckinger A, Delgado JA, Moser S, Moreno L, Neuber B, Grab A, et al. Target expression, generation, preclinical activity, and pharmacokinetics of the BCMA-T cell bispecific antibody EM801 for multiple myeloma treatment. Cancer Cell 2017;31:396–410.
23. Hideshima T, Mitsiades C, Tonon G, Richardson PG, Anderson KC. Understanding multiple myeloma pathogenesis in the bone marrow to identify new therapeutic targets. Nat Rev Cancer 2007;7:585–98.
24. Avet-Loiseau H, Leleu X, Roussel M, Moreau P, Guerin-Charbonnel C, Caillot D, et al. Bortezomib plus dexamethasone induction improves outcome of patients with t(4;14) myeloma but not outcome of patients with del(17p). J Clin Oncol 2010;28:4630–4.
25. Rosinol L, Oriol A, Teruel AI, Hernandez D, Lopez-Jimenez J, de la Rubia J, et al. Superiority of bortezomib, thalidomide, and dexamethasone (VTD) as induction pretransplantation therapy in multiple myeloma: a randomized phase 3 PETHEMA/GEM study. Blood 2012;120:1589–96.
26. Bisping G, Wenning D, Kropff M, Gustavus D, Muller-Tidow C, Stelljes M, et al. Bortezomib, dexamethasone, and fibroblast growth factor receptor 3-specific tyrosine kinase inhibitor in t(4;14) myeloma. Clin Cancer Res 2009;15:520–31.

Published OnlineFirst July 3, 2019; DOI: 10.1158/1535-7163.MCT-18-1216

Molecular Cancer Therapeutics

Anti-GPRC5D/CD3 Bispecific T-Cell–Redirecting Antibody for the Treatment of Multiple Myeloma

Tatsushi Kodama, Yu Kochi, Waka Nakai, et al.

Mol Cancer Ther 2019;18:1555-1564. Published OnlineFirst July 3, 2019.